1 **Article title: MeSSII interplays the amylose and amylopectin biosynthesis by protein**

2 **interactions in cassava storage root**

3 **Running title: Function of starch synthase II in cassava**

4 Shutao He[1,2,3], Xiaomeng Hao[1,3], Shanshan Wang[1,3], Wenzhi Zhou[1], Qiuxiang Ma[1], Xinlu Lu[1],

5 Luonan Chen[2,*], Peng Zhang[1,3,*]

6 [1] National Key Laboratory of Plant Molecular Genetics, CAS Center for Excellence in Molecular

7 Plant Sciences, Institute of Plant Physiology and Ecology, Chinese Academy of Sciences,

8 Shanghai, China

9 [2] Key Laboratory of Systems Biology, CAS Center for Excellence in Molecular Cell Science,

10 Institute of Biochemistry and Cell Biology, Chinese Academy of Sciences, Shanghai, China

11 [3] University of Chinese Academy of Sciences, Beijing, China

12 *** Corresponding authors:**

13 Luonan Chen (lnchen@sibcb.ac.cn) or Peng Zhang (zhangpeng@cemps.ac.cn)

14

15 **One Sentence Summary:** Here, by focusing on cassava SSII, we elucidated its function and the

16 molecular mechanism by which it chaperones the starch synthase complex to regulate starch

17 biosynthesis in cassava storage roots.

18

Abstract: Starch is a glucose polymer synthesized by green plants for energy storage, and is crucial for plant growth and reproduction. The biosynthesis of starch polysaccharides is mediated by members of the large starch synthase (SS) protein superfamily. Here, we showed that in cassava storage roots, soluble starch synthase II (MeSSII) plays an important role in starch biosynthesis via forming protein complexes with other starch biosynthetic enzymes by directly interacting with MeSSI, MeSBEII and MeISAII. The *MeSSII*-RNAi cassava lines showed increased amylose content and reduced intermediate chain of amylopectin (B1 type) biosynthesis in their storage roots, leading to altered starch physico-chemical properties. Further gel permeation chromatography analysis of starch biosynthetic enzymes between the wild type and *MeSSII*-RNAi lines confirmed the key rule of MeSSII in the organization of heteromeric starch synthetic protein complexes, including the MeSSII-MeSSI-MeGBSSI and MeSBEII-MeSSI-MeSSII-MeISAII-MeISAI complexes. The lack of MeSSII in cassava also reduced the binding capacity of the MeSSI, MeSBEII, MeISAI, and MeISAII to starch granules. Our results show a close coordination between granule-bound starch synthase and amylopectin biosynthetic enzymes, which implies that the processes of amylose synthesis and amylopectin synthesis are directly interrelated. These findings shed light on the key components of the starch biosynthesis machinery in root crops.

Keywords: cassava, protein–protein interaction, starch biosynthesis, SSII, storage root

Introduction

Cassava (*Manihot esculenta* Crantz) accumulates large amounts of starch (up to 32% by fresh weight) in its storage roots even under unfavorable growth conditions in tropical and subtropical regions (Cock 1982). Cassava starch is pure white and contains low levels of fat (0.08–1.54%) and proteins (0.03–0.6%), providing an irreplaceable raw material for bioindustrial applications (Li, Cui et al. 2017). Cassava starch granules are generally round and truncated, ranging in size from 5-40 μm, and the amylose content varies from 15% to 30%, depending on the cultivar and growth conditions (Moorthy 2002). Various modified cassava starch derivatives are widely used in the food, textile, paper manufacturing, pharmaceutical, and bioethanol production industries (Zhu 2015). Despite this, the key enzymes and their regulation of starch biosynthesis in cassava storage roots is largely uncharacterized.

Similar to starches from other plant sources, cassava starch in its native form consists of both amylose and amylopectin. Basically, amylose is a largely linear polymer in which glucosyl residues are joined by $\alpha(1\rightarrow4)$ bonds, and is an important and interspersed component of starch, but is not crucial for the spatial structure in the formation of starch granules. Amylopectin is composed of a clustered arrangement of crystalline, densely packed glucosyl residues organized as parallel chains, in which linear α-helices are joined by $\alpha(1\rightarrow4)$ bonds, and interspersed by more disorganized $\alpha(1\rightarrow6)$ branches at regular intervals of ~20-30 glucose units. Such organization

55 eventually forms a classic semicrystalline model that determines the stable and insoluble granular

56 structure of starch (Hizukuri 1986). Typically, branched amylopectin chains are classified as A,

57 with a degree of polymerization (DP) of 6-12, B_1 (DP 13-24), B_2 (DP 25-36), and B_{3+} (DP ≥37)

58 (Hizukuri 1985). The chain length of cassava starch averages 23.2 DP, and the majority consists of

59 up to 43.7% B_1 chains; the molecular weight of native cassava starch varies from 1.885×10^7 to

60 3.323×10^7 g/mol, depending on cultivars and growth conditions (Liu, Zu et al. 2018).

61 Amylose is synthesized by a single enzyme, granule-bound starch synthase (GBSS), and mutants

62 of cassava lacking GBSS produce amylose-free waxy starches (Ceballos, Sanchez et al. 2007,

63 Zhao, Dufour et al. 2011, Bull, Seung et al. 2018). Recent studies have shown that the activity of

64 GBSS can be regulated by post-translational modifications. It was found that in maize, GBSS is

65 phosphorylated in the starch granule (Grimaud, Rogniaux et al. 2008), which is supported by a

66 recent report of rice endosperm GBSS (Liu, Huang et al. 2013). Liu *et al.* (2013) also noted that

67 GBSS can form oligomers, and ATP and protein kinases increase the degree of oligomerization. In

68 addition, with increasing concentrations of ADP-glucose, GBSS oligomerization increases.

69 However, it is still no solid evidence to support whether GBSS associates with amylopectin

70 synthases directly in the plastids.

71 The synthesis of amylopectin, which mainly described from grain seeds, requires the coordinated

72 participation of at least 10 different enzymes, including soluble starch synthases (SSs), starch

73 branching enzymes (BEs or SBEs), and debranching enzymes (DBEs). SSs (EC 2.4.1.21) elongate

74 α-1,4-linked linear glucan polymers using ADP-glucose as a substrate. SBEs (EC 2.4.1.18)

75 produce α-1,6-linked branches and are crucial for amylopectin formation because they are the only

76 enzymes that can form branches in amylopectin. DBEs such as isoamylase (ISA; EC 3.2.1.68) and

77 pullulanase (PUL; EC 3.2.1.41) hydrolyze and remove α-1,6-linked branches, which is essential to

78 organize crystalline structure formation in amylopectin (Nakamura 2002, Jeon, Ryoo et al. 2010).

79 In addition, starch phosphorylase (Pho; EC 2.4.1.1) elongates α-1,4-linked linear glucan polymers

80 using glucose 1-phosphate (G1P) as a substrate, and is thought to be involved in the initiation

81 process of starch biosynthesis (Satoh, Shibahara et al. 2008, Jeon, Ryoo et al. 2010). Although

82 GBSSI has an effect on the extra-long amylopectin chains in addition to participating in amylose

83 synthesis (Hanashiro, Itoh et al. 2008), no direct evidence of its interaction with other amylopectin

84 biosynthetic enzymes has been reported. Recently, starches with remarkably altered

85 physico-chemical properties and amylopectin structure have been observed in transgenic cassava

86 in which the expressions of genes for GBSS1 and SBEs have been silenced (Zhao, Dufour et al.

87 2011, Zhou, Zhao et al. 2020). Nevertheless, the function and regulation of these SSs in cassava

88 remain unclear.

89 Previous studies have shown that SS can interact with SBE isozymes in wheat, maize, barley, and

90 rice seeds (Tetlow, Wait et al. 2004, Hennen-Bierwagen, Liu et al. 2008, Tetlow, Beisel et al. 2008,

91 Liu, Ahmed et al. 2012, Liu, Romanova et al. 2012, Ahmed, Tetlow et al. 2015, Crofts, Abe et al.

2015). In maize, the trimeric complex composed of SSI, SSIIa, and SBEIIb is one of the best studied, and the formation of the trimer depends on protein phosphorylation (Liu, Ahmed et al. 2012, Liu, Romanova et al. 2012, Makhmoudova, Williams et al. 2014, Mehrpouyan, Menon et al. 2020). Protein-protein interactions have also been found between SBEI and SBEIIb, as well as in protein complexes consisting of SSIII, pyruvate orthophosphate dikinase (PPDK), SBEIIb, and AGPase (Hennen-Bierwagen, Lin et al. 2009, Liu, Makhmoudova et al. 2009). In wheat and maize, Pho1 can interact with SBEI and SBEII (Tetlow, Wait et al. 2004, Subasinghe, Liu et al. 2014). Moreover, functional and mutually synergistic relationships between SBEs and Pho1, and SBEs and SSI, have been observed using recombinant rice starch biosynthetic enzymes *in vitro* (Nakamura, Ono et al. 2012, Abe, Asai et al. 2014, Nakamura, Aihara et al. 2014). In addition, there is also the protein-protein interaction between ISA and a carbohydrate-binding module (CBM)-containing protein, FLO6 (Peng, Wang et al. 2014). Recently, GBSSI has been reported to bind to the surface of starch granules by interacting with the PTST protein (Seung, Soyk et al. 2015), and PTST2 also can interact with SSIV to control starch granule initiation in Arabidopsis leaves (Seung, Boudet et al. 2017).

To date, the majority of studies on multi-enzyme complexes have focused on amylopectin synthesis and are limited to the seeds of major gramineous crop species including wheat, barley, maize, and rice. It remains unknown whether there are similar starch synthase complexes in dicotyledonous species and those with underground storage organs. In this study, we found that in cassava, MeSSII affects starch metabolism by forming protein complexes with other starch biosynthetic enzymes. In particular, in contrast to the current dogma, our results showed a close coordination between granule-bound starch synthase (GBSSI) and amylopectin biosynthetic enzymes, which implies that the processes of amylose synthesis and amylopectin synthesis are directly interrelated.

Results

The MeSSII is a member of conserved SSII cluster of starch synthases

Five cassava *SS* genes, which are referred to as *MeSSI*, *MeSSII*, *MeSSIII*, *MeSSIV* and *MeSSV*, were identified after blastp searching the cassava genome using protein sequences of the soluble Arabidopsis starch synthases (SSI to SSV) as queries (Table S1). Phylogenetic analysis of the deduced SS protein sequences from cassava and 15 other plant species showed that the starch synthase protein family can be classified into five categories: the SSI, SSII, SSIII, SSIV, and SSV families (Fig. 1A).

To obtain further insights into the possible structural evolution of the *SSII* genes, the exon-intron structures and conserved domains in these *SSII* genes were visualized using the Gene Structure Display Server (GSDS; http://gsds.cbi.pku.edu.cn/) as shown in Fig. 1B. The numbers of exons varied between 7 and 11. The exon positions also varied between the genes. Although there were

128   various exon-intron patterns present in these species, the conserved domains were found to be
129   highly similar (Fig. 1B). In accordance with previous observations (Liu, Yu et al. 2015, Helle,
130   Bray et al. 2018), all of the deduced SSII proteins were predicted to have Glycos_transf_1 domain
131   and Glyco_transf_5 domain, which are the typical pattern of conserved domains found in the SSII
132   family proteins.

Down-regulated *MeSSII* expression leads to reduced plant growth and biomass in cassava

134   To further investigate the function of MeSSII, we first characterized the tissue-specific gene
135   expression patterns of cassava starch synthase genes in the five SS families (Fig. 1C). Among the
136   5 cassava starch synthase genes, *MeSSV* was almost undetectable in all tissues. In storage roots,
137   *MeSSII* had the highest transcript level among these soluble starch synthase genes, which indicates
138   that *MeSSII* might play an important role in starch metabolism.

139   A 200 bp conserved DNA sequence of cassava *MeSSII* gene (base pairs 978-1177), which encodes
140   the starch synthase catalytic domain, was used as the target sequence for RNAi. After primary
141   growth and phenotypic screening, three *MeSSII*-RNAi transgenic (SSC) plant lines that showed
142   normal growth and development, together with one empty vector (EV) line, were chosen for
143   further study. Single transgene integrations were detected in all transgenic lines by Southern blot
144   analysis using an *HPT* DIG-labeled probe following digestion of genomic DNA with either
145   *Hin*dIII (Fig. 2A, upper panel) or *Eco*RI (Fig. 2A, lower panel). The results of qRT-PCR (Fig. 2B)
146   and Western blotting analyses using antibody against MeSSII (Fig. 2C) suggested that the
147   expression of *MeSSII* in the storage roots of the SSC lines was significantly decreased compared
148   to the wild type (WT) and EV controls.

149   After six months of growth in the field, phenotypic measurements that included plant height,
150   fresh-weight biomass, root number, root length, and root diameter were performed on the WT and
151   transgenic lines. Plant heights ranged from 160.8 cm to 166.6 cm for the SSC lines, which were
152   shorter than both WT and EV line plants (Fig. 2D and Supplementary Fig. S1A). The biomass per
153   plant ranged from 1.39 kg to 2.15 kg for the SSC lines (Fig. 2D and Supplementary Fig. S1B),
154   which was considerably less than the average fresh weight of the WT (4.33 kg) and EV (4.01 kg)
155   plants. The average storage root length was 23.42 cm for WT and 23.33 cm for EV, and it ranged
156   from 19.41 cm to 21.26 cm for the SSC lines (Fig. 2D and Supplementary Fig. S1C). Average root
157   diameter was 2.67 cm for WT, 2.64 cm for EV, and 2.52 cm to 2.88 cm for the SSC lines (Fig. 2D
158   and Supplementary Fig. S1D). The average root number per plant varied from 11.67 to 14 for the
159   SSC lines (Fig. 2D and Supplementary Fig. S1D), which was dramatically less than the numbers
160   for WT (25.1) and EV (25) plants. Thus, for the SSC transgenic lines, total biomass was reduced
161   due to retarded growth of both the aerial and subterranean organs.

MeSSII influences starch properties in cassava storage roots

163   Microscopic analysis of storage root starch granule morphology by SEM and TEM did not show

164 obvious differences between the WT and SSC transgenic lines. The starch in both the WT and SSC

165 lines consisted of a mixture of round, truncated, and dome-shaped granules (Fig. 3A and

166 Supplementary Fig. S2). The starch granule size distributions in the SSC transgenic lines differed

167 from those of the WT and EV. The SSC lines exhibited a broader granule size distribution

168 compared to the WT and EV, and contained a greater number of larger starch granules which were

169 largely responsible for the increased average granule size in the SSC lines (Fig. 3B).

170 The relative proportion of amylose was dramatically increased in the SSC lines compared with

171 starch from the WT and EV (Fig. 3C). In the SSC lines, the number of chains with DP 6-9 and DP

172 24-40 increased, while the number of chains with DP 10-23 decreased (Fig. 3D). The chain length

173 distribution (CLD) differential patterns in the SSC lines indicated that MeSSII could play a key

174 role in the synthesis of short to intermediate length amylopectin chains (DP 10-23) in cassava

175 storage roots.

176 RVA analysis showed that root starches from the SSC lines exhibited different pasting patterns

177 compared to WT and EV starches (Fig. 3E). The pasting temperature (PT) of WT starch was

178 71.05°C, while all three SSC starches showed increased PTs (Table S2). Overall, the values for

179 peak viscosity (PV), hot paste viscosity (HV), breakdown (BD), final viscosity (FV), and setback

180 (SB) were significantly lower in the SSC lines than in starches from the WT and EV lines. The

181 DSC (differential scanning calorimeter) parameters of the starch samples were determined in order

182 to evaluate the gelatinization properties (Table S3). Starch isolated from WT roots gelatinized with

183 a temperature range of 56.26°C (T_o) to 78.21°C (T_c) and an enthalpy ($\triangle H$) of 11 J/g. The

184 gelatinization temperatures (T_o, T_p, and T_c) and enthalpies ($\triangle H$) were decreased in starch isolated

185 from the SSC transgenic lines, and showed clear differences when compared with starches from

186 the WT and EV lines.

187 X-ray diffraction (XRD) analysis of normal cassava storage starch showed typical A-type crystals

188 with one doublet around 17° (2θ) and two singlets predominantly around 15° and 23° (2θ) (Fig. 3F)

189 (Zhao, Dufour et al. 2011). Compared to storage root starch from WT and EV plants, SSC storage

190 starches underwent pronounced changes in their diffraction patterns, including replacement of a

191 doublet with a singlet emerging around 17° (2θ). The peak intensities around 15°, 17°, and 23° (2θ)

192 of SSC starches were weaker than that of WT and EV starches.

193 **No obvious alternations in protein levels of six key starch biosynthetic enzymes**

194 First, we obtained polyclonal antibodies specific for cassava MeSSI, MeSSII, MeSBEI, MeSBEII,

195 MeISAI, MeISAII and MeGBSSI by means of recombinant protein immunization. Genetic tests to

196 verify the specificity of each antiserum by using RNAi transgenic plants including SSC-6, *sbe1*

197 (Zhou, Zhao et al. 2020), *sbe2* (Zhou, Zhao et al. 2020) and *gbss1* (Zhao, Dufour et al. 2011),

198 which inhibit expression levels of *MeSSII*, *MeSBEI*, *MeSBEII* and *MeGBSSI*, respectively. The

199 results demonstrate conclusively that all these antibodies had good specificity and could

200   specifically recognize the corresponding proteins (Supplementary Fig. S3).

201   Subsequently, the above antibodies were used to analyze the expression and solubility of starch
202   biosynthetic enzymes from cassava mature roots (diameter > 2.5 cm) by immunoblotting. Proteins
203   were extracted using a denaturing buffer which also gelatinizes the starch to enable extraction of
204   granule-bound proteins. The results showed that all of these enzymes (MeSSI, MeSSII, MeSBEI,
205   MeSBEII, MeISAI, MeISAII, and MeGBSSI) can be detected in the soluble part (Supplementary
206   Fig. S4). Generally, MeGBSSI binds to starch granules tightly and is not soluble, but in our
207   analysis, 51% of the MeGBSSI could be detected in the soluble fraction in the cassava storage
208   roots.

209   To further uncover how MeSSII reduction affects starch properties, the relative mRNA levels of
210   other six key starch biosynthetic genes were determined by qRT-PCR (Supplementary Fig. S5A).
211   Although only *MeSSI* and *MeSBEII* transcription was found to be up-regulated in the SSC lines,
212   all six enzymes showed no significant differences at protein levels in the SSC lines compared to
213   the WT and EV (Supplementary Fig. S5B). These results indicate that the phenotypic differences
214   between the transgenic SSC lines and WT are not due to the expression of these six starch
215   biosynthetic genes.

216   **MeSSII forms protein complexes with other starch biosynthetic enzymes**

217   To illustrate the molecular weight distribution patterns of seven key starch biosynthetic enzymes
218   (MeSSI, MeSSII, MeSBEI, MeSBEII, MeISAI, MeISAII and MeGBSSI), soluble proteins
219   extracted from mature cassava storage roots were fractionated using gel permeation
220   chromatography (GPC) and blue native polyacrylamide gel electrophoresis (BN-PAGE). All seven
221   enzymes were detected in the higher molecular weight fraction (Fig. 4A, B), which is consistent
222   with the notion that they can form protein complexes.

223   To investigate possible interacting partners among these starch biosynthetic isozymes,
224   immunoprecipitation was performed by using soluble cassava storage root protein extracts and
225   isozyme-specific antibodies (Fig. 4C). The results demonstrated that the pairwise protein
226   interactions obtained by reciprocal co-immunoprecipitation includes MeSSI-MeSSII,
227   MeSSI-MeSBEI, MeSSI-MeSBEII, MeSSI-MeISAI, MeSSI-MeISAII, MeGBSSI-MeSSI,
228   MeSSII-MeSBEII, MeSSII-MeGBSSI, MeSBEI-MeISAI, MeSBEI-MeISAII, MeSBEI-MeGBAII,
229   MeSBEII-MeISAII,   MeISAI-MeISAII,   MeISAI-MeISAII,   MeISAI-MeISAII,   and
230   MeISAI-MeISAII.   Western   blot   signals   obtained   from   only   one   side   of   the
231   co-immunoprecipitation included AbMeSSII-MeSBEI, AbMeSSII-MeISAI, AbMeSSII-MeISAII,
232   AbMeSBEI-MeSBEII,   and   AbMeISAII-MeGBSSI   (first   acronym,   antibody   used   for
233   immunoprecipitation; second acronym, isozyme detected by Western blotting).

234   To further explore the components of the starch biosynthetic isozyme complexes in mature
235   cassava storage roots, protein complexes immunoprecipitated by each antibody were analyzed

236   separately by LC-MS/MS, and the identified proteins are summarized in Table S4. The results

237   showed that MeSSI, MeSSII, MeSBEI, MeSBEII, MeISAI, MeISAII, and MeGBSSI can be

238   co-immunoprecipitated by each antibody, indicating that these enzymes form protein complexes

239   through specific protein-protein interactions, further confirming the Co-IP experiment results (Fig.

240   4C). In addition, many other proteins were also detected. Among these proteins, the 14-3-3 protein

241   was co-immunoprecipitated by each antibody. Starch phosphorylase (MePho) can be

242   co-immunoprecipitated with MeSBEI and MeSBEII antibodies, which is consistent with previous

243   reports showing that Pho can interact with SBEI and SBEII (Tetlow, Wait et al. 2004, Subasinghe,

244   Liu et al. 2014). MePho is also co-immunoprecipitated by antibodies against MeSSI, MeSSII,

245   MeISAI, MeISAII, and MeGBSSI. Pyruvate orthophosphate dikinase (MePPDK) can be

246   co-immunoprecipitated with MeSSII and MeGBSSI, which is consistent with previous reports that

247   PPDK can form protein complexes with starch biosynthetic enzymes (Hennen-Bierwagen, Lin et

248   al. 2009). Furthermore, each antibody can co-immunoprecipitate with MeAGPase and MeSuS.

249   To investigate direct protein-protein interaction patterns among these seven enzymes, we

250   performed yeast-two-hybrid (Y2H) assays. We found that MeSSI, MeSSII, and MeSBEII can

251   interact with one another (Fig. 5A). MeSSII can interact with itself and MeISAII directly, and the

252   interaction between MeSSII and MeISAII was a very interesting finding, indicating that SSs,

253   SBEs and ISAs may assemble into multi-enzymes complexes to perform their functions.

254   Furthermore, we found that MeGBSSI could interact with itself and was also capable of

255   interacting with MeSSI and MeISAI (Fig. 5A). In addition, we detected strong interactions

256   between MeISAI and MeISAII, and MeISAII with itself.

257   The Y2H results were validated by testing these interactions in bimolecular fluorescence

258   complementation (BiFC) experiments. The cDNAs encoding the above seven enzymes were

259   cloned into BiFC vectors to generate protein fusions with either the N-terminal half of YFP (nYFP)

260   or the C-terminal half of YFP (cYFP). Vector combinations of nYFP-MeSSI+cYFP-MeSSII,

261   nYFP-MeSSI+cYFP-MeSBEII, nYFP-MeSSI+cYFP-MeGBSSI, nYFP-MeSSII+cYFP-MeSBEII,

262   nYFP-MeSSII+cYFP-MeISAII,   nYFP-MeISAI+cYFP-MeISAII,   and

263   nYFP-MeISAI+cYFP-MeGBSSI were transiently co-expressed in *N. benthamiana* leaves, and

264   strong YFP fluorescence signals were detected in the chloroplasts (Fig. 5B and Supplementary Fig.

265   S6), which were consistent with the Y2H results (Fig. 5A).

266   **MeSSII influences GPC mobility and granule-bound ability of starch biosynthetic enzymes**

267   To investigate whether the absence of MeSSII would alter the GPC mobility of other members of

268   the complex, soluble proteins extracted from mature roots of the WT and SSC lines were

269   fractionated using GPC (Fig. 6A). MeSSI and MeSBEII mobility in the GPC column was

270   significantly affected by the absence of MeSSII. In the WT protein extract, MeSBEII was not

271   detected in the 232 kDa fraction, and the amount of MeSSI present in the 232 kDa fraction was

272   reduced compared with the SSC lines. No obvious changes in the GPC mobility of other proteins

273   (MeSBEI, MeISAI, MeISAII, and MeGBSSI) were detected in the SSC lines compared with WT.

274   The fact that MeSSI and MeSBEII exhibited altered GPC elution volumes when MeSSII was

275   depleted, compared with WT, is consistent with the proposal that the three proteins associate with

276   one another in the same quaternary structure.

277   Furthermore, to investigate the effect of MeSSII on starch granule-bound protein, granule-bound

278   proteins isolated from starch samples extracted from storage roots of WT and the SSC lines were

279   detected by Western blotting (Fig. 6B). MeSSI, MeSBEII, MeISAI, and MeISAII were not

280   detected in the SSC lines, although they were present as granule-bound proteins in WT, whereas

281   no differences were observed in the granule-bound protein profiles for MeSBEI and MeGBSSI

282   between WT and the SSC lines.

283   **Discussion**

284   At present, all members of the starch synthase family in plants are classified into seven

285   subfamilies that include GBSS, SSI, SSII, SSIII, SSIV, SSV, and SSVI based on the earliest

286   available genomic sequences (Yang, Wang et al. 2013, Helle, Bray et al. 2018, Abt, Pfister et al.

287   2020), and mainly limited to Arabidopsis and economically important crop species. The functions

288   of six starch synthases, including GBSSI, SSI, SSII, SSIII, SSIV, and SSV have been

289   well-documented in previous studies (Craig, Lloyd et al. 1998, Edwards, Fulton et al. 1999,

290   Kossmann, Abel et al. 1999, McPherson and Jane 1999, Song and Jane 2000, Yamamori, Fujita et

291   al. 2000, Fulton, Edwards et al. 2002, Yoo and Jane 2002, Morell, Kosar-Hashemi et al. 2003,

292   Delvalle, Dumez et al. 2005, Nakamura, Francisco et al. 2005, Fujita, Yoshida et al. 2006, Fujita,

293   Yoshida et al. 2007, Roldan, Wattebled et al. 2007, Ryoo, Yu et al. 2007, Zhang, Szydlowski et al.

294   2008, Takahata, Tanaka et al. 2010, Zhao, Dufour et al. 2011, Zhou, Wang et al. 2016, Wang, Li et

295   al. 2017, Abt, Pfister et al. 2020). It has been demonstrated that amylopectin biosynthetic isozymes

296   can interact with each other in the endosperms of wheat, maize, barley, and rice seeds (Tetlow,

297   Wait et al. 2004, Hennen-Bierwagen, Liu et al. 2008, Tetlow, Beisel et al. 2008,

298   Hennen-Bierwagen, Lin et al. 2009, Liu, Makhmoudova et al. 2009, Ahmed, Tetlow et al. 2015,

299   Crofts, Abe et al. 2015). Also, amylose synthase GBSSI is also able to form oligomers in rice, and

300   GBSSI activity and oligomerization are affected by phosphorylation, redox regulation, and ADPG

301   (Liu, Huang et al. 2013). Nevertheless, these knowledges are limited to the seeds of the major

302   gramineous crop species. It is still unclear whether similar starch synthase complexes are present

303   in dicotyledonous species and in underground storage organs. In this study, by focusing on cassava

304   SSII, we have elucidated its function and the molecular mechanism by which it chaperones the

305   starch synthase complex to regulate starch biosynthesis in cassava storage roots (Figs. 2-6,

306   Supplementary Fig. S1-2 and Table S2-3). Based on our findings and those of previously

307   published studies (Hennen-Bierwagen, Lin et al. 2009, Crofts, Abe et al. 2015), we propose a

308   functional model of MeSSII that uncovers new features of starch biosynthesis in dicot plants,

309   especially in root crops (Fig. 7).

310   Further investigation showed that MeSSII is important for growth and development in cassava
311   (Fig. 2D and Supplementary Fig. S1), and the starch isolated from storage roots of the
312   *MeSSII*-RNAi lines showed altered physico-chemical properties, such as amylose content, pasting,
313   gelatinization properties, and crystallinity (Fig. 3 and Supplementary Fig. S2 and Table S2-3),
314   indicating that MeSSII plays a vital role in starch biosynthesis in cassava. Among these properties,
315   the increased amylose content in roots of the SSC lines is an interesting phenomenon (Fig. 3C),
316   and implies that as an amylopectin synthase, MeSSII has an important influence on amylose
317   synthesis. Analyses of the mRNA and protein expression levels of key enzymes involved in starch
318   synthesis demonstrated that the effect of MeSSII on starch biosynthesis was not achieved by
319   affecting the expression levels of the genes that encode these enzymes (Supplementary Fig. S5A,
320   B). Our results show that MeSSII influenced the ability of MeSSI, MeSBEII, MeISAI, and
321   MeISAII to bind to starch granules (Fig. 6B), which is similar to the effect of cereal SSIIa on the
322   ability of SSI and SBEII to bind to starch granule (Yamamori, Fujita et al. 2000, Morell,
323   Kosar-Hashemi et al. 2003, Umemoto and Aoki 2005), although the presence of a carbohydrate
324   binding module was not predicted in MeSSII (Fig. 1B). This indicates that MeSSII may bind to
325   starch granules by interacting with other proteins that contain a CBM domain. Furthermore,
326   obvious changes in the GPC mobility of MeSSI and MeSBEII in the *MeSSII*-RNAi lines also
327   implies the significance of MeSSII in these protein complexes that consist of starch biosynthetic
328   enzymes (Fig. 6A). Therefore, we propose that owing to the disruption of these protein complexes,
329   a deficiency in MeSSII affects the starch binding ability of other key enzymes in starch synthesis
330   and even might influence the activity of these enzymes, leading to a significant alteration in starch
331   properties.

332   In this study, we have confirmed the presence of multienzyme complexes for starch biosynthesis
333   in cassava storage roots, a dicot species. The results of our study also revealed
334   previously-unknown protein interactions among starch biosynthetic enzymes in plants. Although
335   protein-protein interactions among SSs including GBSSI have been reported (Liu, Huang et al.
336   2013, Crofts, Abe et al. 2015, Seung, Soyk et al. 2015), it is still unclear whether GBSSI
337   participates in amylopectin synthesis. Here, we found that MeGBSSI can interact with MeSSI and
338   MeISAI directly (Fig. 5A, B), strongly implying that GBSSI is directly involved in the process of
339   amylopectin synthesis. With regard to the function of the interactions between MeGBSSI and
340   MeSSI or MeISAI, GBSSI may interact with amylopectin enzymatic complexes through SSI, and
341   contribute to the synthesis of extra-long amylopectin chains directly, as shown in previous studies
342   in potato and rice (Fulton, Edwards et al. 2002, Hanashiro, Itoh et al. 2008). Furthermore, GBSSI
343   may interact with SBEII through SSI to produce more branches in amylose and the extra-long
344   amylopectin chains, leading to the synthesis of more amylopectin clusters. It should also be noted
345   that pea amylose was reported to be debranched completely by isoamylase (ISA) in aqueous 40%
346   dimethyl sulfoxide (Colonna and Mercier 1984). The interaction between GBSSI and ISAI
347   indicates that ISAI may excise the extra erroneous branched chains in amylopectin in favor of

348   producing long chains or the synthesis of amylose by interacting with GBSSI. In *Chlamydomonas*
349   *reinhardtii*, amylose can be formed by extending the branches on amylopectin, which are then
350   removed from the amylopectin chains (van de Wal, D'Hulst et al. 1998). The interaction between
351   GBSSI and the amylopectin enzymatic complexes through SSI might play a role in regulating the
352   activity of one another. In wheat, SSI, SSII, SBEIIa, or SBEIIb can form heterotrimers after
353   phosphorylation of SBEIIa or SBEIIb, which increases the enzymatic activity of SBEIIa and
354   SBEIIb significantly (Tetlow, Beisel et al. 2008). In addition, PhoI can improve the activity of
355   SBE by interacting with SBE in rice (Crofts, Abe et al. 2015).

356   To date, a direct interaction between ISAs and the protein complexes that consist of SS and SBE
357   has not been reported. The removal of erroneous branches by ISAs plays an important role in the
358   extension and branching of amylopectin chains, and, therefore, protein interactions with ISAs are
359   essential (Hussain, Mant et al. 2003, Delatte, Trevisan et al. 2005, Kubo, Colleoni et al. 2010,
360   Utsumi, Utsumi et al. 2011, Peng, Wang et al. 2014). Lin *et al.* (2012) hypothesized that ISAI may
361   interact with SSIII, either directly or indirectly, so that ISAI can bind to the growing amylopectin
362   molecules (Lin, Huang et al. 2012). The interaction between ISA and a CBM-containing FLO6
363   protein shows that ISA could potentially bind to starch granules via FLO6 (Peng, Wang et al.
364   2014). In cassava, we found that MeSSII can interact with MeISAII directly (Fig. 5A, B),
365   suggesting that MeISAI and MeISAII are part of the protein complexes that consist of SS and SBE
366   via their interactions with MeSSII, and hence, contributing directly to amylopectin synthesis by
367   removing the erroneous branches.

368   In conclusion, we elucidated the function of MeSSII in starch biosynthesis in cassava storage roots.
369   Our work describes a new mechanism of starch accumulation in underground storage organs of a
370   dicot species. Contrary to current dogma, our results suggest that starch synthesis requires a close
371   coordination between GBSSI and amylopectin biosynthetic enzymes, and that amylose synthesis
372   and amylopectin synthesis are directly interrelated. Further molecular investigations into the
373   regulatory mechanisms of starch biosynthesis in cassava, such as the transcription factors that
374   regulate the expression of the genes that encode these enzymes, will improve our understanding of
375   the mechanisms governing starch accumulation in cassava storage roots. Additionally, this work
376   provides a novel source of cassava starch with a high amylose content for various industrial
377   applications.

378   **Materials and methods**

379   **Phylogenetic tree analysis of starch synthases**

380   Arabidopsis (*Arabidopsis thaliana*) SSI, SSII, SSIII, SSIV, and SSV sequences were retrieved
381   from Phytozome and the closest orthologs in the other species, including *Amborella trichopoda*,
382   *Brachypodium distachyon*, *Capsella rubella*, *Chlamydomonas reinhardtii*, *Glycine max*,
383   *Gossypium raimondii*, *Hordeum vulgare*, *Manihot esculenta*, *Oryza sativa*, *Populus trichocarpa*,

384 *Physcomitrella patens*, *Prunus persica*, *Sorghum bicolor*, *Vitis vinifera* and *Zea mays*, were
385 obtained from the Phytozome and Ensembl Plants via BLASTp. The three closest prokaryotic
386 glycogen synthase sequences of AtSSIII, At-SSIV, and At-SSV (WP 048672006.1, WP
387 059061331.1, and WP026046064.1, respectively) were retrieved from the National Center for
388 Biotechnology Information as an outgroup. We aligned sequences using MUSCLE (Edgar 2004)
389 with the default parameters that are tuned for accuracy. A phylogenetic tree was created by
390 MEGA7, using the maximum likelihood method with the Jones-Taylor-Thornton matrix-based
391 model (Jones, Taylor et al. 1992). Bootstrap values were obtained with 1,000 replications.
392 Positions with less than 95% site coverage were eliminated. The exon-intron structure and
393 conserved amino acid domains of these SSII genes was determined by the Gene Structure Display
394 Server (GSDS: http://gsds.gao-lab.org/index.php).

MeSSII cloning and production of MeSSII-RNAi transgenic cassava

396 Sequence information for *MeSSII* was derived from the cassava genome database
397 (http://www.phytozome.net). The full length cDNA of *MeSSII* was cloned from a cassava cDNA
398 library. The binary RNAi gene silencing expression vector p35S::*MeSSII*-RNAi was constructed
399 from the plasmid pRNAi-dsAC1 (Vanderschuren, Alder et al. 2009). The AC1 sequence was
400 excised and replaced with a partial *MeSSII* cDNA sequence from 978 bp to 1177 bp. The control
401 construct was pRNAi-dsAC1 without the *MeSSII* cDNA. The two constructs were introduced into
402 *Agrobacterium tumefaciens* LBA4404 and the cassava cultivar TMS60444 was used to generate
403 transgenic plants as described previously by Zhang *et al.* (2000) (Zhang, Potrykus et al. 2000).
404 The integration pattern of T-DNA in transgenic cassava was determined by Southern blot analysis
405 as described by Zhao *et al.* (2011) (Zhao, Dufour et al. 2011). The DIG-labeled hygromycin
406 phosphotransferase (HPT) gene was used as the hybridization probe.

407 The regenerated transgenic lines and WT plants were propagated *in vitro* and then transferred to
408 pots in the greenhouse for macro-propagation (16 h/8 h of light/dark, 30°C/22°C day/night). The
409 *MeSSII*-RNAi transgenic lines are given the designation SSC, which is an abbreviation for the
410 "starch synthase catalytic domain" used for constructing the p35S::*MeSSII*-RNAi vector, and the
411 control lines are designated EV, which is the abbreviation for "empty vector". For field evaluation,
412 10 stems per transgenic line and WT were planted in early May in the Wushe Plantation for
413 Transgenic Crops, Shanghai, China (31°13948.0099 N, 121°28912.0099E), and harvested in early
414 November. The phenotypic performance of the plants was recorded.

Transcriptional and translational expression analysis

416 Leaves, petioles, stems, and storage roots from at least three plants per line were harvested and
417 then ground to a fine powder in liquid N_2 for mRNA extraction. To quantify the expression of
418 genes, qRT-PCR was performed as described (Xu, Duan et al. 2013). The *β-Actin* gene was used
419 as a reference to normalize gene expression. The sequences of the PCR primers used in these

420   experiments are shown in Table S5.

421   Protein extraction was performed as described by Crofts *et al.* (2015) (Crofts, Abe et al. 2015)

422   with some modifications. Mature cassava storage roots (diameter >2.5 cm; 1 g samples) were used

423   for each extraction. Total protein was extracted with 1 vol (w/v) of a denaturing buffer containing

424   0.125 M Tris-HCl (pH 6.8), 8 M urea, 4% SDS, and 5% β-mercaptoethanol. Samples were

425   extracted overnight at room temperature, centrifuged at 12,000 rpm to remove gelatinized starch

426   and other particulate matter, and the supernatants were used for denaturing polyacrylamide gel

427   electrophoresis (SDS-PAGE) and immunoblotting. Soluble proteins were extracted on ice with 6

428   vols (w/v) (three repeats with 2 vols each) of an extraction buffer containing 10 mM HEPES-KOH

429   (pH 7.5) and 100 mM NaCl. After extraction, samples were centrifuged at 12,000 rpm at 4°C for

430   15 min. The residual pellet was extracted with 1 vol (w/v) of denaturing buffer as described above,

431   centrifuged as before, and the supernatant was then used to represent the insoluble, starch

432   granule-associated proteins.

433   Proteins were transferred to polyvinylidene fluoride (PVDF) membranes after SDS-PAGE or blue

434   native (BN)-PAGE. Membranes were treated as described by Crofts *et al.* (2015) (Crofts, Abe et al.

435   2015). Polyclonal antibodies against MeSSI, MeSSII, MeSBEI, MeSBEII, MeISAI, MeISAII, and

436   MeGBSSI were prepared by ABclonal Biotech Co., Ltd using purified recombinant proteins

437   (purity >95%) as antigens. Primary antibodies were used at a dilution of 1:1,000. HRP-conjugated

438   goat anti-rabbit IgG (Sigma) was used as a secondary antibody at a dilution of 1:10,000. The

439   colorimetric signal was detected with the Pierce ECL Western Blotting Substrate Reagent Kit

440   (catalog no. 32106; Thermo Fisher) and was visualized using the Tanon-5500 Chemiluminescent

441   Imaging System (Tanon Science and Technology, Shanghai, China).

442   **Physico-chemical property assays of cassava storage starches**

443   The granule size distribution of starch extracted from cassava storage roots was determined as

444   described by Zhou *et al.* (2015) (Zhou, Yang et al. 2015). A Mastersizer 2000 laser diffraction

445   instrument (Malvern Instruments Ltd., Worcestershire, UK) was used in wet-well mode. The

446   starch was added to the reservoir and sonicated for 30 s at 6 W until an obscuration value of 12-17%

447   was reached. The refractive indices used for the water and starch were 1.330 and 1.50, respectively.

448   The particle size distributions are presented as the diameter versus volume. To examine whether

449   starch granule morphology was altered in the different transgenic lines, the starch granules were

450   coated with gold after they were spread on a metal stub and then observed under a scanning

451   electron microscope (SEM, JSM6360lv, JEOL, Tokyo, Japan). Pieces of fresh mature roots (2

452   mm^3) were coated with 1,3-diformal propane and subjected to ultra-thin sectioning. The sections

453   were then photographed under a transmission electron microscope (TEM; Hitachi H7650, Tokyo,

454   Japan).

455   The chain length distribution (CLD) of the starches was measured as described by Zhou *et al.*

456 (2015) (Zhou, Yang et al. 2015). Starch from the transgenic plants and WT was digested with
457 *Pseudomonas amyloderamosa* isoamylase (Sigma), and the CLD of the amylopectin was analyzed
458 using high-performance anion-exchange chromatography with pulsed amperometric detection
459 (HPAEC-PAD; Dionex-ICS 3000; Dionex Corporation, USA). A D8 Advance Bruker X-ray
460 diffractometer (Bruker AXS, Germany) was used to study the crystal type of the starch granules.
461 Starch powders were scanned with the 2θ diffraction angle at 4-50°. The crystal patterns and
462 degree of crystallinity were analyzed using Jade 5.0 software.

463 The thermal properties of the starch samples were determined using a differential scanning
464 calorimeter (DSC Q2000; TA Instrument Ltd., UK). A mixture of starch and distilled water (w/w,
465 1:3) was sealed in an aluminum pan and scanned at 10°C/min from 30°C to 95°C with an empty
466 aluminum pan as a reference. The gelatinization temperature and enthalpy were calculated using
467 Universal Analysis 2000 software. The pasting properties of the starch were analyzed using a rapid
468 viscosity analyzer (model RVA-Super 3; Newport Scientific Pty. Ltd., Australia). The starch was
469 suspended in distilled water (5% w/v, dry weight basis) and tested using a dedicated program for
470 cassava. The temperature of the starch slurry was increased from 30°C to 95°C at a rate of
471 5°C/min and held at 95°C for 6 min, followed by cooling to 50°C at the same rate, and the
472 temperature was maintained at 50°C for 10 min. The rotating speed of the paddle was 960 rpm
473 during the first 10 s, after which it was kept constant (160 rpm) throughout the analysis.

474 The amylose content of the starch was measured using colorimetric amylose content determination
475 as previously described (Knutson and Grove 1994). Amylose (Type III, Sigma A0512, St. Louis,
476 MO) and amylopectin (Sigma 10118) from potato were used to establish standard curves.

477 **Analysis of protein interactions**

478 Samples of cassava storage roots (1.5 g) were extracted in 1.5 ml of gel filtration buffer containing
479 50 mM Tris-acetate (pH 7.5), 100 mM NaCl, 10 μl/ml plant protease inhibitor cocktail
480 (Sigma-Aldrich LLC) and centrifuged at 12,000 rpm for 15 min. The supernatants were injected
481 into a 500 μl sample loop, and fractionated by gel permeation chromatography (GPC) using a
482 Superdex 200 10/300 GL column (GE Healthcare, catalog no. 17-5175-01) connected to an AKTA
483 FPLC system (GE Healthcare) at 4°C. The column was equilibrated with 50 mM Tris-acetate
484 buffer (pH 7.5) containing 100 mM NaCl; the flow rate was 1 ml/min and fraction sizes of 0.5 ml
485 were collected. Molecular mass standards run under identical conditions were from GE Healthcare
486 (catalog no. 17-0445-01). Samples from each fraction (40 μl) were analyzed by SDS-PAGE and
487 immunoblotting.

488 The BN-PAGE procedures used in this study were performed as previously described (Crofts et al.,
489 2015) (Crofts, Abe et al. 2015) with some modifications. Cassava storage roots were extracted
490 with 1 vol (w/v) of 50 mM Bis-Tris (pH 7.5), 50 mM NaCl, 10% glycerol, 0.001% Ponceau S, and
491 centrifuged at 12,000 × g for 10 min. The supernatants were subjected to 3-12% acrylamide

492   Bis-Tris native-PAGE (Invitrogen, catalog no. BN1001BOX) and electrophoresed with an anode

493   buffer containing 50 mM Bis-Tris and 50 mM tricine, and a cathode buffer containing 50 mM

494   Bis-Tris, 50 mM tricine and 0.004% CBB G-250 stain at 80 V for an initial 1 h and at 120 V for

495   the remaining time.

496   Co-immunoprecipitation experiments were performed using the methods described by Liu *et al.*

497   (2012) (Liu, Ahmed et al. 2012). Purified peptide-specific antibodies (each approximately 2 μg)

498   were individually used for the co-immunoprecipitation (Co-IP) experiments with the soluble

499   protein extracts described above (1 ml, between 0.8 and 1.2 mg/ml protein). The protein

500   extract/antibody mixtures were incubated at room temperature on a rotator for 50 min, and

501   immunoprecipitation of the antibody/protein complexes was performed by adding 50 μl of Protein

502   A-Sepharose (Sigma-Aldrich) made up as a 50% (w/v) slurry with phosphate buffered saline (PBS;

503   137 mM NaCl, 10 mM Na_2HPO_4, 2.7 mM KCl, 1.8 M KH_2PO_4, pH 7.4) at room temperature for

504   40 min. The Protein A-Sepharose/antibody/protein complexes were recovered by centrifugation at

505     $2,000 \times g$ for 5 min at 4°C in a refrigerated microcentrifuge, and the supernatants were discarded.

506   The pellets were washed five times with PBS (1.3 ml each), followed by washing five times with a

507   buffer containing 10 mM HEPES-NaOH (pH 7.5) and 150 mM NaCl. The washed pellets were

508   boiled in SDS-containing gel loading buffer and separated by SDS-PAGE, followed by

509   immunoblot analysis. In order to exclude the possibility that co-immunoprecipitation of the

510   proteins observed in the immunoprecipitation pellet was a result of AGPL, AGPS, SS, SBE, ISA

511   or GBSS binding to the same glucan chain, the soluble protein extracts used for

512   immunoprecipitation were pre-incubated with 5 U each of the glucan degrading enzymes

513   amyloglucosidase (EC 3.2.1.3, Sigma A7255) and α-amylase (EC 3.2.1.1, Sigma A2643) for 20

514   min at 25°C.

515   Yeast two-hybridization (Y2H) assays were performed according to the manufacture's procedure

516   (Clontech Laboratories Inc., Palo Alto, CA, USA). For each isozyme, a DNA fragment that was

517   PCR-amplified using the specific primer pair (Table S1) was cloned in-frame into pGBKT7 to

518   form the bait construct. The same fragment was inserted into pGADT7 to form the prey construct.

519   Both plasmids were transformed into yeast cells (strain AH109). The resulting yeast transformants

520   were grown on SD medium containing 3-AT and X-α-gal, but lacking Trp, Leu, His, and Ade, for

521   2-3 days at 30°C.

522   Bimolecular fluorescence complementation was conducted as previously described (Ma, Kong et

523   al. 2015) with some modifications. Each starch biosynthetic enzyme cDNA was introduced into

524   BiFC vectors enabling protein fusions to the N-terminal half of YFP or C-terminal half of YFP

525   (nYFP-fused and cYFP-fused, respectively). nYFP-fused with cYFP-fused, nYFP-fused with

526   cYFP, nYFP with cYFP-fused, or nYFP-cYFP cDNAs were transiently co-produced in *N.*

527   *benthamiana* leaves. Confocal images of *N. benthamiana* epidermal cells transiently co-expressing

528   these cDNAs are used to analyze these interactions here. The primers used in these experiments

529   are shown in Table S5.

Mass spectrometry

531   The proteins were digested in the gel with bovine trypsin as previously described (Wang, Li et al.
532   2007). After digestion, the peptides were collected and detected by LC-MS/MS according to the
533   facility procedures used at the Public Mass Spectrometry Technical Service Center, CAS Center
534   for Excellence in Molecular Plant Sciences, Chinese Academy of Sciences. Data were analyzed
535   using Proteome Discoverer software.

Statistical analysis

537   Root samples were collected from three independent plants per line. Data from at least three
538   replicates are presented as mean ± SD. Analysis of independent samples with Student's t-test was
539   performed using SPSS software, version 17 (SPSS Inc., Chicago, IL, USA). An alpha value of P
540   <0.05 was considered to be statistically significant.

Author contributions

550   S.H. performed most of the experiments, analyzed the data, and drafted the manuscript; X.H.,
551   S.W., and W.Z. conducted some of the experiments; S.W. and Q.M. produced the transgenic
552   cassava plants; X.H., Q.M. and X.L. maintained the transgenic cassava plants; P.Z., L.C., S.H.
553   designed and conceived this project; P.Z. and L.C. analyzed the data and revised the manuscript
554   with input from the other authors. All authors contributed to and approved the final manuscript.

References

556   Abe, N., H. Asai, H. Yago, N. F. Oitome, R. Itoh, N. Crofts, Y. Nakamura and N. Fujita (2014).
557   "Relationships between starch synthase I and branching enzyme isozymes determined using double
558   mutant rice lines." Bmc Plant Biology **14**.
559   Abt, M. R., B. Pfister, M. Sharma, S. Eicke, L. Burgy, I. Neale, D. Seung and S. C. Zeeman (2020).
560   "STARCH SYNTHASE5, a Noncanonical Starch Synthase-Like Protein, Promotes Starch Granule Initiation
561   in Arabidopsis." Plant Cell **32**(8): 2543-2565.
562   Ahmed, Z., I. J. Tetlow, R. Ahmed, M. K. Morell and M. J. Emes (2015). "Protein-protein interactions
563   among enzymes of starch biosynthesis in high-amylose barley genotypes reveal differential roles of

564 heteromeric enzyme complexes in the synthesis of A and B granules." Plant Sci **233**: 95-106.

565 Bull, S. E., D. Seung, C. Chanez, D. Mehta, J. E. Kuon, E. Truernit, A. Hochmuth, I. Zurkirchen, S. C.
566 Zeeman, W. Gruissem and H. Vanderschuren (2018). "Accelerated ex situ breeding of GBSS- and
567 PTST1-edited cassava for modified starch." Sci Adv **4**(9): eaat6086.

568 Ceballos, H., T. Sanchez, N. Morante, M. Fregene, D. Dufour, A. M. Smith, K. Denyer, J. C. Perez, F. Calle
569 and C. Mestres (2007). "Discovery of an amylose-free starch mutant in cassava (Manihot esculenta
570 Crantz)." J Agric Food Chem **55**(18): 7469-7476.

571 Cock, J. H. (1982). "Cassava: a basic energy source in the tropics." Science **218**(4574): 755-762.

572 Colonna, P. and C. Mercier (1984). "Macromolecular Structure of Wrinkled-Pea and Smooth-Pea Starch
573 Components." Abstracts of Papers of the American Chemical Society **188**(Aug): 59-Carb.

574 Craig, J., J. R. Lloyd, K. Tomlinson, L. Barber, A. Edwards, T. L. Wang, C. Martin, C. L. Hedley and A. M.
575 Smith (1998). "Mutations in the gene encoding starch synthase II profoundly alter amylopectin
576 structure in pea embryos." Plant Cell **10**(3): 413-426.

577 Crofts, N., N. Abe, N. F. Oitome, R. Matsushima, M. Hayashi, I. J. Tetlow, M. J. Emes, Y. Nakamura and N.
578 Fujita (2015). "Amylopectin biosynthetic enzymes from developing rice seed form enzymatically active
579 protein complexes." J Exp Bot **66**(15): 4469-4482.

580 Delatte, T., M. Trevisan, M. L. Parker and S. C. Zeeman (2005). "Arabidopsis mutants Atisa1 and Atisa2
581 have identical phenotypes and lack the same multimeric isoamylase, which influences the branch
582 point distribution of amylopectin during starch synthesis." Plant Journal **41**(6): 815-830.

583 Delvalle, D., S. Dumez, F. Wattebled, I. Roldan, V. Planchot, P. Berbezy, P. Colonna, D. Vyas, M.
584 Chatterjee, S. Ball, A. Merida and C. D'Hulst (2005). "Soluble starch synthase I: a major determinant for
585 the synthesis of amylopectin in Arabidopsis thaliana leaves." Plant J **43**(3): 398-412.

586 Edgar, R. C. (2004). "MUSCLE: multiple sequence alignment with high accuracy and high throughput."
587 Nucleic Acids Res **32**(5): 1792-1797.

588 Edwards, A., D. C. Fulton, C. M. Hylton, S. A. Jobling, M. Gidley, U. Rossner, C. Martin and A. M. Smith
589 (1999). "A combined reduction in activity of starch synthases II and III of potato has novel effects on
590 the starch of tubers." Plant Journal **17**(3): 251-261.

591 Fujita, N., M. Yoshida, N. Asakura, T. Ohdan, A. Miyao, H. Hirochika and Y. Nakamura (2006). "Function
592 and characterization of starch synthase I using mutants in rice." Plant Physiology **140**(3): 1070-1084.

593 Fujita, N., M. Yoshida, T. Kondo, K. Saito, Y. Utsumi, T. Tokunaga, A. Nishi, H. Satoh, J. H. Park, J. L. Jane,
594 A. Miyao, H. Hirochika and Y. Nakamura (2007). "Characterization of SSIIIa-deficient mutants of rice:
595 the function of SSIIIa and pleiotropic effects by SSIIIa deficiency in the rice endosperm." Plant Physiol
596 **144**(4): 2009-2023.

597 Fulton, D. C., A. Edwards, E. Pilling, H. L. Robinson, B. Fahy, R. Seale, L. Kato, A. M. Donald, P.
598 Geigenberger, C. Martin and A. M. Smith (2002). "Role of granule-bound starch synthase in
599 determination of amylopectin structure and starch granule morphology in potato." J Biol Chem
600 **277**(13): 10834-10841.

601 Grimaud, F., H. Rogniaux, M. G. James, A. M. Myers and V. Planchot (2008). "Proteome and
602 phosphoproteome analysis of starch granule-associated proteins from normal maize and mutants
603 affected in starch biosynthesis." J Exp Bot **59**(12): 3395-3406.

604 Hanashiro, I., K. Itoh, Y. Kuratomi, M. Yamazaki, T. Igarashi, J. I. Matsugasako and Y. Takeda (2008).
605 "Granule-bound starch synthase I is responsible for biosynthesis of extra-long unit chains of
606 amylopectin in rice." Plant and Cell Physiology **49**(6): 925-933.

607 Helle, S., F. Bray, J. Verbeke, S. Devassine, A. Courseaux, M. Facon, C. Tokarski, C. Rolando and N.

608 Szydlowski (2018). "Proteome Analysis of Potato Starch Reveals the Presence of New Starch Metabolic
609 Proteins as Well as Multiple Protease Inhibitors." Frontiers in Plant Science **9**.

610 Hennen-Bierwagen, T. A., Q. Lin, F. Grimaud, V. Planchot, P. L. Keeling, M. G. James and A. M. Myers
611 (2009). "Proteins from multiple metabolic pathways associate with starch biosynthetic enzymes in
612 high molecular weight complexes: a model for regulation of carbon allocation in maize amyloplasts."
613 Plant Physiol **149**(3): 1541-1559.

614 Hennen-Bierwagen, T. A., F. Liu, R. S. Marsh, S. Kim, Q. Gan, I. J. Tetlow, M. J. Emes, M. G. James and A.
615 M. Myers (2008). "Starch biosynthetic enzymes from developing maize endosperm associate in
616 multisubunit complexes." Plant Physiol **146**(4): 1892-1908.

617 Hizukuri, S. (1985). "Relationship between the Distribution of the Chain-Length of Amylopectin and
618 the Crystalline-Structure of Starch Granules." Carbohydrate Research **141**(2): 295-306.

619 Hizukuri, S. (1986). "Polymodal Distribution of the Chain Lengths of Amylopectins, and Its
620 Significance." Carbohydrate Research **147**(2): 342-347.

621 Hussain, H., A. Mant, R. Seale, S. Zeeman, E. Hinchliffe, A. Edwards, C. Hylton, S. Bornemann, A. M.
622 Smith, C. Martin and R. Bustos (2003). "Three isoforms of isoamylase contribute different catalytic
623 properties for the debranching of potato glucans." Plant Cell **15**(1): 133-149.

624 Jeon, J. S., N. Ryoo, T. R. Hahn, H. Walia and Y. Nakamura (2010). "Starch biosynthesis in cereal
625 endosperm." Plant Physiol Biochem **48**(6): 383-392.

626 Jones, D. T., W. R. Taylor and J. M. Thornton (1992). "The rapid generation of mutation data matrices
627 from protein sequences." Comput Appl Biosci **8**(3): 275-282.

628 Knutson, C. A. and M. J. Grove (1994). "Rapid Method for Estimation of Amylose in Maize Starches."
629 Cereal Chemistry **71**(5): 469-471.

630 Kossmann, J., G. J. W. Abel, F. Springer, J. R. Lloyd and L. Willmitzer (1999). "Cloning and functional
631 analysis of a cDNA encoding a starch synthase from potato (Solanum tuberosum L,) that is
632 predominantly expressed in leaf tissue." Planta **208**(4): 503-511.

633 Kubo, A., C. Colleoni, J. R. Dinges, Q. Lin, R. R. Lappe, J. G. Rivenbark, A. J. Meyer, S. G. Ball, M. G.
634 James, T. A. Hennen-Bierwagen and A. M. Myers (2010). "Functions of heteromeric and homomeric
635 isoamylase-type starch-debranching enzymes in developing maize endosperm." Plant Physiol **153**(3):
636 956-969.

637 Li, S., Y. Cui, Y. Zhou, Z. Luo, J. Liu and M. Zhao (2017). "The industrial applications of cassava: current
638 status, opportunities and prospects." J Sci Food Agric **97**(8): 2282-2290.

639 Lin, Q. H., B. Q. Huang, M. X. Zhang, X. L. Zhang, J. Rivenbark, R. L. Lappe, M. G. James, A. M. Myers
640 and T. A. Hennen-Bierwagen (2012). "Functional Interactions between Starch Synthase III and
641 Isoamylase-Type Starch-Debranching Enzyme in Maize Endosperm." Plant Physiology **158**(2): 679-692.

642 Liu, D. R., W. X. Huang and X. L. Cai (2013). "Oligomerization of rice granule-bound starch synthase 1
643 modulates its activity regulation." Plant Sci **210**: 141-150.

644 Liu, F., Z. Ahmed, E. A. Lee, E. Donner, Q. Liu, R. Ahmed, M. K. Morell, M. J. Emes and I. J. Tetlow (2012).
645 "Allelic variants of the amylose extender mutation of maize demonstrate phenotypic variation in
646 starch structure resulting from modified protein-protein interactions." J Exp Bot **63**(3): 1167-1183.

647 Liu, F., N. Romanova, E. A. Lee, R. Ahmed, M. Evans, E. P. Gilbert, M. K. Morell, M. J. Emes and I. J.
648 Tetlow (2012). "Glucan affinity of starch synthase IIa determines binding of starch synthase I and
649 starch-branching enzyme IIb to starch granules." Biochem J **448**(3): 373-387.

650 Liu, F. S., A. Makhmoudova, E. A. Lee, R. Wait, M. J. Emes and I. J. Tetlow (2009). "The amylose
651 extender mutant of maize conditions novel protein-protein interactions between starch biosynthetic

652   enzymes in amyloplasts." Journal of Experimental Botany **60**(15): 4423-4440.

653   Liu, H., G. Yu, B. Wei, Y. Wang, J. Zhang, Y. Hu, Y. Liu, G. Yu, H. Zhang and Y. Huang (2015).
654   "Identification and Phylogenetic Analysis of a Novel Starch Synthase in Maize." Front Plant Sci **6**: 1013.

655   Liu, K., Y. Y. Zu, C. D. Chi, B. Gu, L. Chen and X. X. Li (2018). "Modulation of the digestibility and
656   multi-scale structure of cassava starch by controlling the cassava growth period." International Journal
657   of Biological Macromolecules **120**: 346-353.

658   Ma, W., Q. Kong, M. Grix, J. J. Mantyla, Y. Yang, C. Benning and J. B. Ohlrogge (2015). "Deletion of a
659   C-terminal intrinsically disordered region of WRINKLED1 affects its stability and enhances oil
660   accumulation in Arabidopsis." Plant J **83**(5): 864-874.

661   Makhmoudova, A., D. Williams, D. Brewer, S. Massey, J. Patterson, A. Silva, K. A. Vassall, F. Liu, S.
662   Subedi, G. Harauz, K. W. Siu, I. J. Tetlow and M. J. Emes (2014). "Identification of multiple
663   phosphorylation sites on maize endosperm starch branching enzyme IIb, a key enzyme in amylopectin
664   biosynthesis." J Biol Chem **289**(13): 9233-9246.

665   McPherson, A. E. and J. Jane (1999). "Comparison of waxy potato with other root and tuber starches."
666   Carbohydrate Polymers **40**(1): 57-70.

667   Mehrpouyan, S., U. Menon, I. J. Tetlow and M. J. Emes (2020). "Protein Phosphorylation Regulates
668   Maize Endosperm Starch Synthase IIa Activity and Protein-Protein Interactions." Plant J.

669   Moorthy, S. N. (2002). "Physicochemical and functional properties of tropical tuber starches: A
670   review." Starch-Starke **54**(12): 559-592.

671   Morell, M. K., B. Kosar-Hashemi, M. Cmiel, M. S. Samuel, P. Chandler, S. Rahman, A. Buleon, I. L. Batey
672   and Z. Y. Li (2003). "Barley sex6 mutants lack starch synthase IIa activity and contain a starch with
673   novel properties." Plant Journal **34**(2): 172-184.

674   Nakamura, Y. (2002). "Towards a better understanding of the metabolic system for amylopectin
675   biosynthesis in plants: Rice endosperm as a model tissue." Plant and Cell Physiology **43**(7): 718-725.

676   Nakamura, Y., S. Aihara, N. Crofts, T. Sawada and N. Fujita (2014). "In vitro studies of enzymatic
677   properties of starch synthases and interactions between starch synthase I and starch branching
678   enzymes from rice." Plant Science **224**: 1-8.

679   Nakamura, Y., P. B. Francisco, Y. Hosaka, A. Sato, T. Sawada, A. Kubo and N. Fujita (2005). "Essential
680   amino acids of starch synthase IIa differentiate amylopectin structure and starch quality between
681   japonica and indica rice varieties." Plant Molecular Biology **58**(2): 213-227.

682   Nakamura, Y., M. Ono, C. Utsumi and M. Steup (2012). "Functional Interaction Between Plastidial
683   Starch Phosphorylase and Starch Branching Enzymes from Rice During the Synthesis of Branched
684   Maltodextrins." Plant and Cell Physiology **53**(5): 869-878.

685   Peng, C., Y. Wang, F. Liu, Y. Ren, K. Zhou, J. Lv, M. Zheng, S. Zhao, L. Zhang, C. Wang, L. Jiang, X. Zhang,
686   X. Guo, Y. Bao and J. Wan (2014). "FLOURY ENDOSPERM6 encodes a CBM48 domain-containing
687   protein involved in compound granule formation and starch synthesis in rice endosperm." Plant J **77**(6):
688   917-930.

689   Roldan, I., F. Wattebled, M. Mercedes Lucas, D. Delvalle, V. Planchot, S. Jimenez, R. Perez, S. Ball, C.
690   D'Hulst and A. Merida (2007). "The phenotype of soluble starch synthase IV defective mutants of
691   Arabidopsis thaliana suggests a novel function of elongation enzymes in the control of starch granule
692   formation." Plant J **49**(3): 492-504.

693   Ryoo, N., C. Yu, C. S. Park, M. Y. Baik, I. M. Park, M. H. Cho, S. H. Bhoo, G. An, T. R. Hahn and J. S. Jeon
694   (2007). "Knockout of a starch synthase gene OsSSIIIa/Flo5 causes white-core floury endosperm in rice
695   (Oryza sativa L.)." Plant Cell Rep **26**(7): 1083-1095.

696 Satoh, H., K. Shibahara, T. Tokunaga, A. Nishi, M. Tasaki, S. K. Hwang, T. W. Okita, N. Kaneko, N. Fujita,
697 M. Yoshida, Y. Hosaka, A. Sato, Y. Utsumi, T. Ohdan and Y. Nakamura (2008). "Mutation of the plastidial
698 alpha-glucan phosphorylase gene in rice affects the synthesis and structure of starch in the
699 endosperm." Plant Cell **20**(7): 1833-1849.

700 Seung, D., J. Boudet, J. Monroe, T. B. Schreier, L. C. David, M. Abt, K. J. Lu, M. Zanella and S. C.
701 Zeemana (2017). "Homologs of PROTEIN TARGETING TO STARCH Control Starch Granule Initiation in
702 Arabidopsis Leaves." Plant Cell **29**(7): 1657-+.

703 Seung, D., S. Soyk, M. Coiro, B. A. Maier, S. Eicke and S. C. Zeeman (2015). "PROTEIN TARGETING TO
704 STARCH Is Required for Localising GRANULE-BOUND STARCH SYNTHASE to Starch Granules and for
705 Normal Amylose Synthesis in Arabidopsis." Plos Biology **13**(2).

706 Song, Y. and J. Jane (2000). "Characterization of barley starches of waxy, normal, and high amylose
707 varieties." Carbohydrate Polymers **41**(4): 365-377.

708 Subasinghe, R. M., F. Liu, U. C. Polack, E. A. Lee, M. J. Emes and I. J. Tetlow (2014). "Multimeric states
709 of starch phosphorylase determine protein-protein interactions with starch biosynthetic enzymes in
710 amyloplasts." Plant Physiol Biochem **83**: 168-179.

711 Takahata, Y., M. Tanaka, M. Otani, K. Katayama, K. Kitahara, O. Nakayachi, H. Nakayama and M.
712 Yoshinaga (2010). "Inhibition of the expression of the starch synthase II gene leads to lower pasting
713 temperature in sweetpotato starch." Plant Cell Rep **29**(6): 535-543.

714 Tetlow, I. J., K. G. Beisel, S. Cameron, A. Makhmoudova, F. Liu, N. S. Bresolin, R. Wait, M. K. Morell and
715 M. J. Emes (2008). "Analysis of protein complexes in wheat amyloplasts reveals functional interactions
716 among starch biosynthetic enzymes." Plant Physiology **146**(4): 1878-1891.

717 Tetlow, I. J., R. Wait, Z. Lu, R. Akkasaeng, C. G. Bowsher, S. Esposito, B. Kosar-Hashemi, M. K. Morell
718 and M. J. Emes (2004). "Protein phosphorylation in amyloplasts regulates starch branching enzyme
719 activity and protein-protein interactions." Plant Cell **16**(3): 694-708.

720 Umemoto, T. and N. Aoki (2005). "Single-nucleotide polymorphisms in rice starch synthase IIa that
721 alter starch gelatinisation and starch association of the enzyme." Functional Plant Biology **32**(9):
722 763-768.

723 Utsumi, Y., C. Utsumi, T. Sawada, N. Fujita and Y. Nakamura (2011). "Functional Diversity of Isoamylase
724 Oligomers: The ISA1 Homo-Oligomer Is Essential for Amylopectin Biosynthesis in Rice Endosperm."
725 Plant Physiology **156**(1): 61-77.

726 van de Wal, M., C. D'Hulst, J. P. Vincken, A. Buleon, R. Visser and S. Ball (1998). "Amylose is synthesized
727 in vitro by extension of and cleavage from amylopectin." Journal of Biological Chemistry **273**(35):
728 22232-22240.

729 Vanderschuren, H., A. Alder, P. Zhang and W. Gruissem (2009). "Dose-dependent RNAi-mediated
730 geminivirus resistance in the tropical root crop cassava." Plant Mol Biol **70**(3): 265-272.

731 Wang, X., X. Li, X. Deng, H. Han, W. Shi and Y. Li (2007). "A protein extraction method compatible with
732 proteomic analysis for the euhalophyte Salicornia europaea." Electrophoresis **28**(21): 3976-3987.

733 Wang, Y., Y. Li, H. Zhang, H. Zhai, Q. Liu and S. He (2017). "A soluble starch synthase I gene, IbSSI, alters
734 the content, composition, granule size and structure of starch in transgenic sweet potato." Sci Rep **7**(1):
735 2315.

736 Xu, J., X. Duan, J. Yang, J. R. Beeching and P. Zhang (2013). "Enhanced reactive oxygen species
737 scavenging by overproduction of superoxide dismutase and catalase delays postharvest physiological
738 deterioration of cassava storage roots." Plant Physiol **161**(3): 1517-1528.

739 Yamamori, M., S. Fujita, K. Hayakawa, J. Matsuki and T. Yasui (2000). "Genetic elimination of a starch

740 granule protein, SGP-1, of wheat generates an altered starch with apparent high amylose." Theoretical
741 and Applied Genetics **101**(1-2): 21-29.

742 Yang, Z., Y. Wang, S. Xu, C. Xu and C. Yan (2013). "Molecular evolution and functional divergence of
743 soluble starch synthase genes in cassava (manihot esculenta crantz)." Evol Bioinform Online **9**:
744 239-249.

745 Yoo, S. H. and J. L. Jane (2002). "Structural and physical characteristics of waxy and other wheat
746 starches." Carbohydrate Polymers **49**(3): 297-305.

747 Zhang, P., I. Potrykus and J. Puonti-Kaerlas (2000). "Efficient production of transgenic cassava using
748 negative and positive selection." Transgenic Res **9**(6): 405-415.

749 Zhang, X., N. Szydlowski, D. Delvalle, C. D'Hulst, M. G. James and A. M. Myers (2008). "Overlapping
750 functions of the starch synthases SSII and SSIII in amylopectin biosynthesis in Arabidopsis." BMC Plant
751 Biol **8**: 96.

752 Zhao, S. S., D. Dufour, T. Sanchez, H. Ceballos and P. Zhang (2011). "Development of waxy cassava with
753 different Biological and physico-chemical characteristics of starches for industrial applications."
754 Biotechnol Bioeng **108**(8): 1925-1935.

755 Zhou, H., L. Wang, G. Liu, X. Meng, Y. Jing, X. Shu, X. Kong, J. Sun, H. Yu, S. M. Smith, D. Wu and J. Li
756 (2016). "Critical roles of soluble starch synthase SSIIIa and granule-bound starch synthase Waxy in
757 synthesizing resistant starch in rice." Proc Natl Acad Sci U S A **113**(45): 12844-12849.

758 Zhou, W., J. Yang, Y. Hong, G. Liu, J. Zheng, Z. Gu and P. Zhang (2015). "Impact of amylose content on
759 starch physicochemical properties in transgenic sweet potato." Carbohydr Polym **122**: 417-427.

760 Zhou, W., S. Zhao, S. He, Q. Ma, X. Lu, X. Hao, H. Wang, J. Yang and P. Zhang (2020). "Production of
761 very-high-amylose cassava by post-transcriptional silencing of branching enzyme genes." J Integr Plant
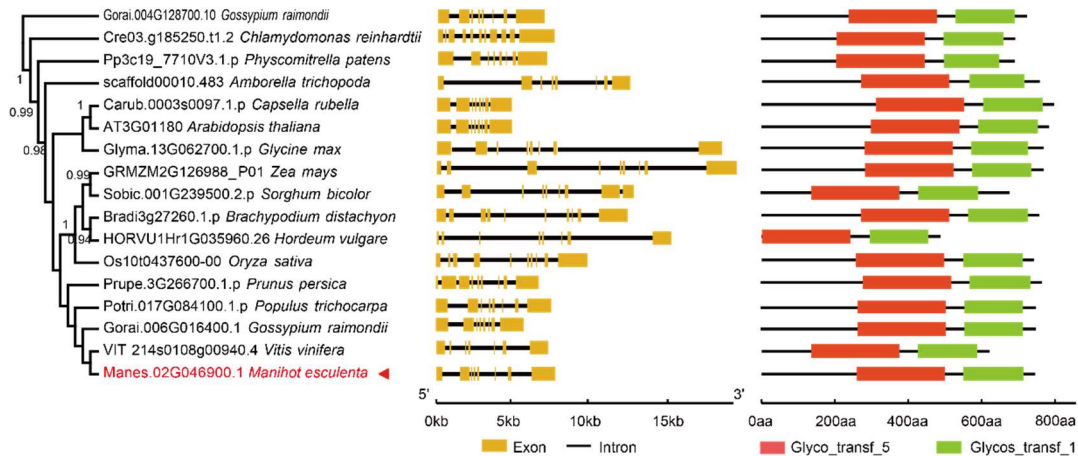762 Biol **62**(6): 832-846.

763 Zhu, F. (2015). "Composition, structure, physicochemical properties, and modifications of cassava
764 starch." Carbohydr. Polym **122**: 456-480.

765

766
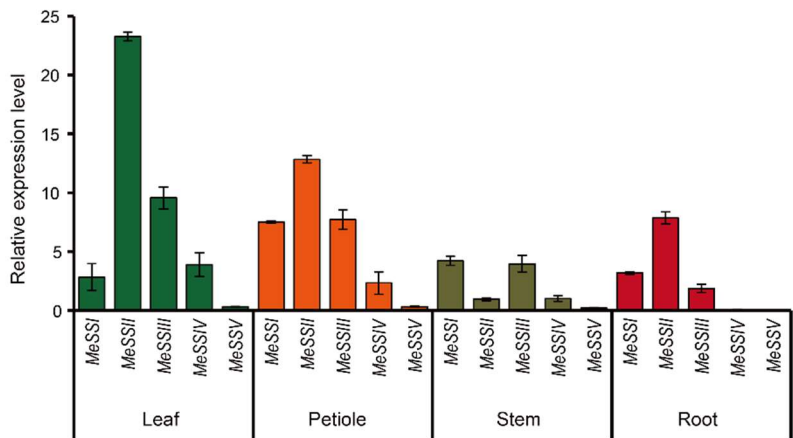
767   **Figure 1**

A
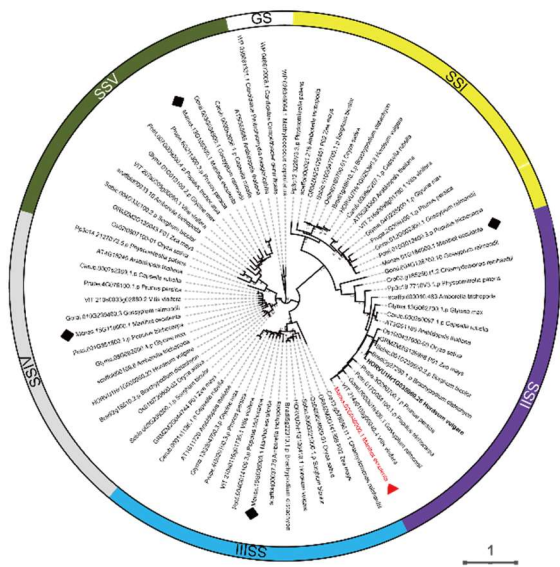
B

C

768

769   **Figure 1. Molecular phylogenies of the plant soluble starch synthase families and**

770   **transcription of soluble starch synthase genes in cassava.**

771   **(A)** Molecular phylogenies of the plant soluble starch synthase families calculated using the

22 / 33

772   maximum likelihood method as implemented in MEGA7. Cassava SSs are marked with a black

773   rhombus (MeSSI, MeSSIII, MessIV and MeSSV) and a red triangle (MeSSII). The closest

774   prokaryotic sequences of At-SS3, At-SS4, and At-SS5 (GS) were included as an outgroup to root

775   the phylogeny.

776   **(B)** Phylogenetic tree, gene structure, and domain analyses of soluble starch synthase II (SSII)

777   proteins. The phylogenetic tree of SSIIs constructed with MEGA using the maximum likelihood

778   method is shown in the left panel. Exon-intron structures of *SSII* genes are shown in the middle

779   panel. Conserved domains annotated using the Pfam database are shown on the right panel.

780   Glyco_transf_1, Glycosyl transferases group 1; Glyco_transf_5, starch synthase catalytic domain.

781   The numbers on the nodes show the bootstrap values.

782   **(C)** mRNA levels of transcribed soluble starch synthase genes in different cassava organs

783   quantified by qRT-PCR assays.

784

785 **Figure 2**
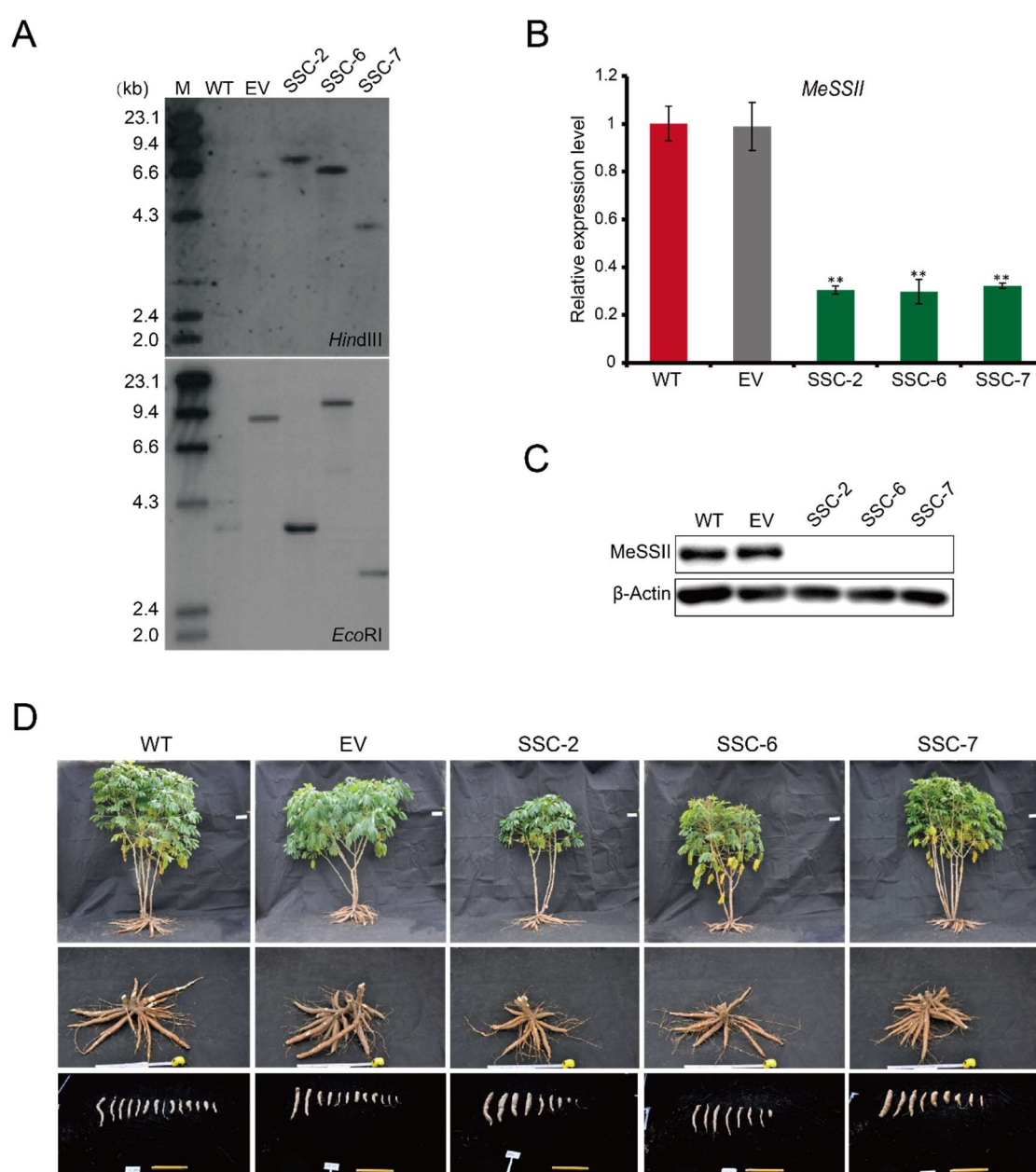
786

787 **Figure 2. Repression of MeSSII expression affects phenotypes of field-grown cassava.**

788 **(A)** Integration patterns of transgenes in SSC transgenic cassava plant lines determined by
789 Southern blotting analysis. M, DIG-labeled molecular marker; WT, wild type control; EV, empty
790 vector plasmid 35::RNAi; SSC-x, plant lines transformed with 35S::MeSSII-RNAi.

791 **(B-C)** mRNA (B) and protein (C) levels of *MeSSII* in storage roots of wild type (WT), empty
792 vector (EV) and *MeSSII*-RNAi (SSC) transgenic plants determined by qRT-PCR and Western
793 blotting using a specific antibody against MeSSII, respectively. The actin protein was used as a
794 loading control.

795 **(D)** Canopy architecture (upper panel), attached storage roots (middle panel), and harvested

796   storage roots (lower panel) of the SSC transgenic plants in comparison with the wild type (WT)

797   and empty vector (EV) plants.

798

800
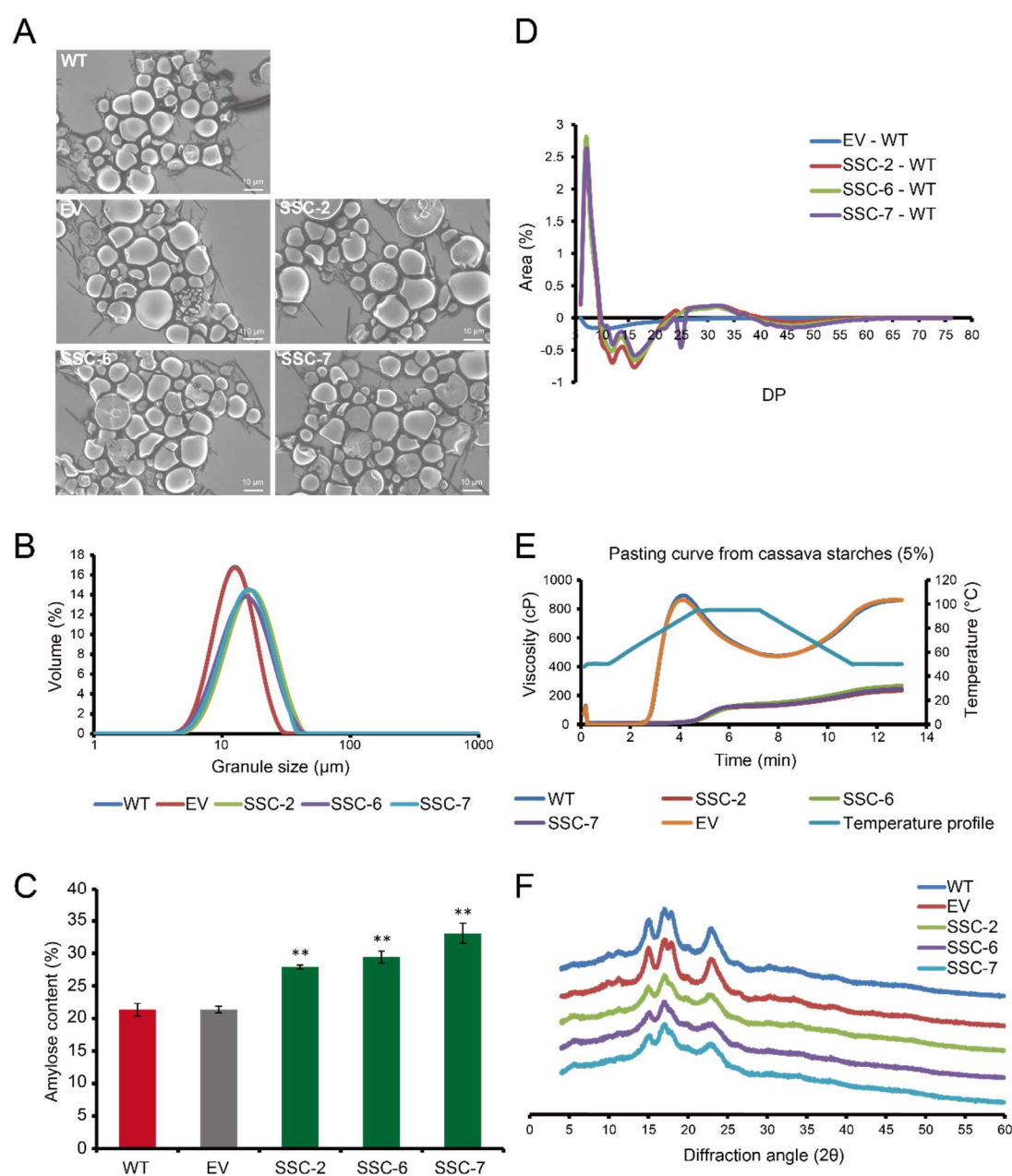
Figure 3. Physico-chemical properties of storage root starches in cassava.

(A, B) Scanning electron microscopy (A) and starch granule size distribution (B) of starch granules from wild type (WT), empty vector (EV), and SSC transgenic cassava plants.

(C-E) Amylose content (C), Chain length distribution (D), Rapid Visco Analyser (RVA) pasting profiles (E), and X-ray diffractograms (F) of storage starches isolated from plants of WT, EV, and SSC transgenic plant lines. * and ** indicate a significant difference compared to WT at $P < 0.05$ and < 0.01, respectively, determined by Student's t-test.

808

Figure 4

810
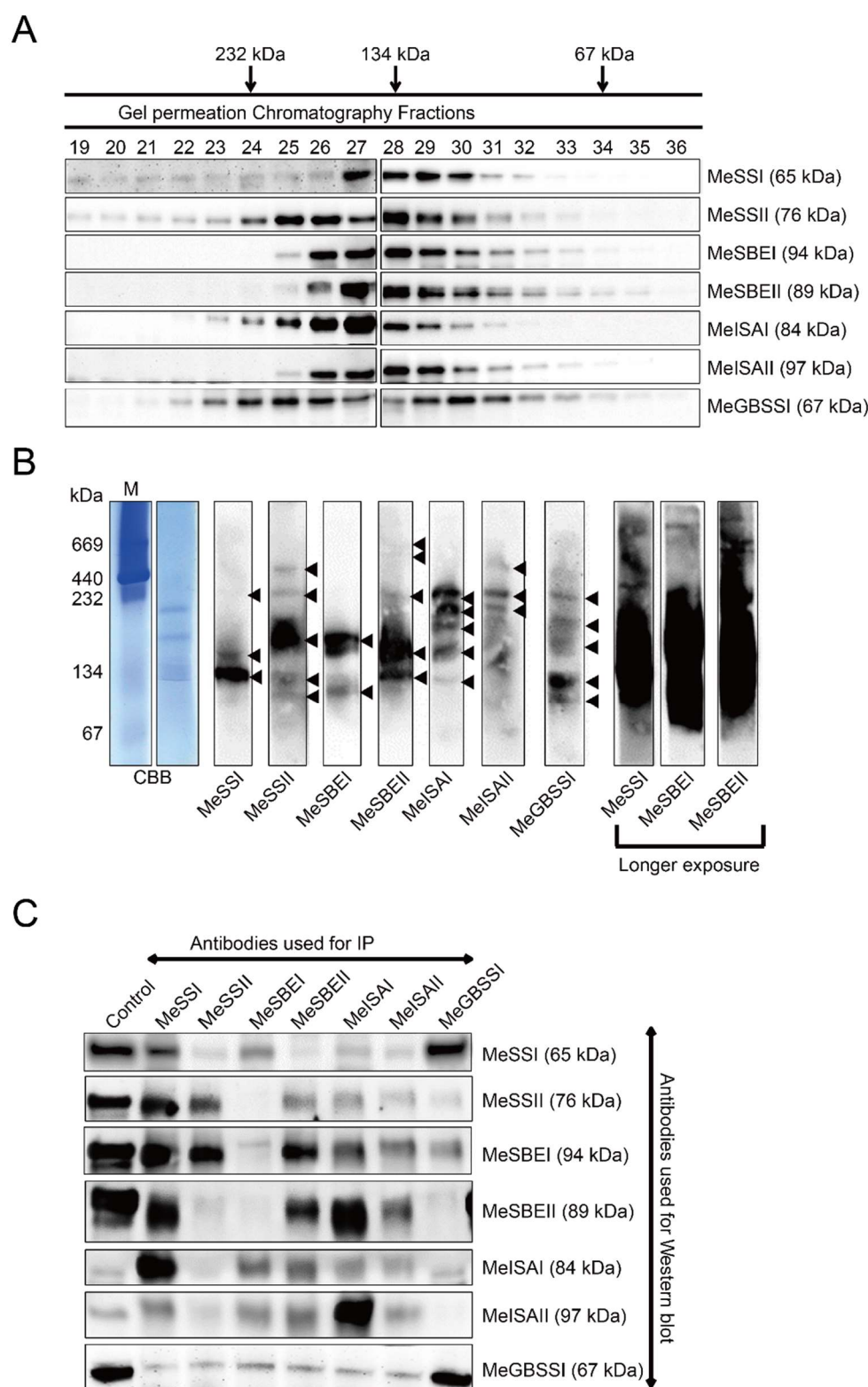
Figure 4. Protein-protein interactions among starch biosynthetic enzymes of cassava.

**(A)** GPC analyses of proteins extracted from mature storage roots of wild type (WT) cassava. Proteins present in the indicated fractions from the GPC column were separated by SDS-PAGE

814   and then probed with each specific antibody in immunoblot analyses. The peak elution volumes of

815   molecular mass standards analyzed using the same GPC protocol are indicated at the top.

816   Monomeric molecular weights of each enzyme are indicated on the right.

817   **(B)** Blue native (BN)-PAGE analyses of starch biosynthetic enzyme complexes from mature

818   storage roots of wild type (WT) cassava. Soluble protein extracts were separated by native-PAGE

819   and then stained with Coomassie brilliant blue (CBB) or probed with specific antibodies in

820   immunoblot analyses. Arrowheads indicate the presence of polypeptides recognized by the

821   antibodies.

822   **(C)** Co-immunoprecipitation (Co-IP) analyses of cassava starch biosynthetic enzymes. Soluble

823   proteins from mature storage roots were immunoprecipitated using the corresponding specific

824   antibodies. Soluble proteins from WT cassava storage roots were used as a positive control. The

825   antibodies used for Western blotting are indicated on the right.

826
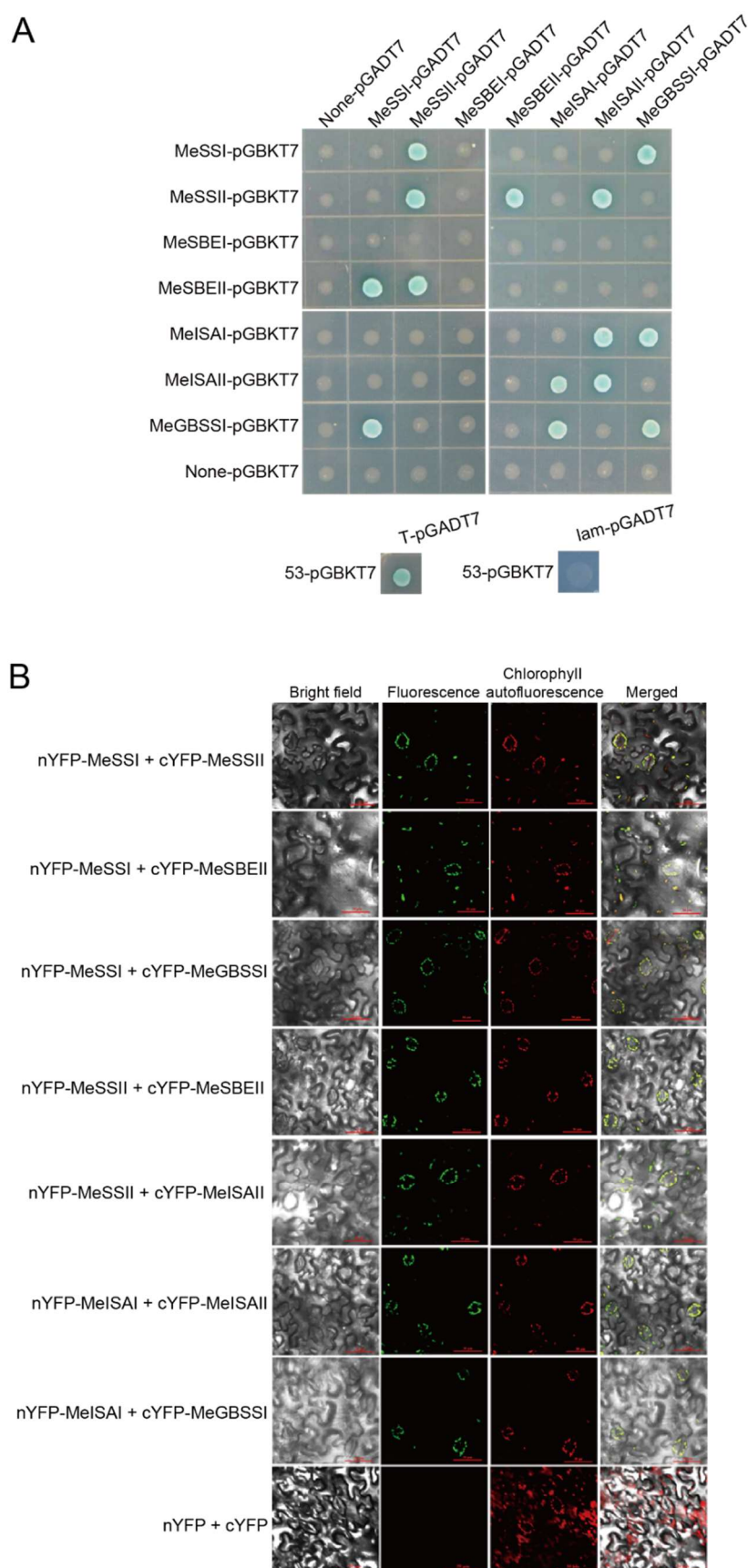
827   **Figure 5**

828

830 **cassava.**

831 **(A)** Yeast two-hybrid analyses. Empty vectors (None-pGBKT7 and None-pGADT7) were used as

832 the negative control. 53-pGBKT7/T-pGADT7 was used as the positive control, and

833 53-pGBKT7/lam-pGADT7 was used as the negative control.

834 **(B)** Bimolecular fluorescence complementation (BiFC) assays. The empty vectors (nYFP+cYFP)
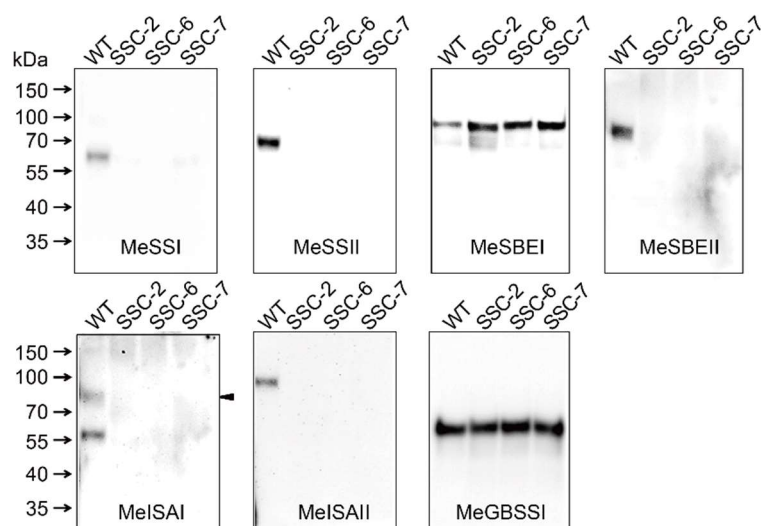
835 were used as a negative control.

836
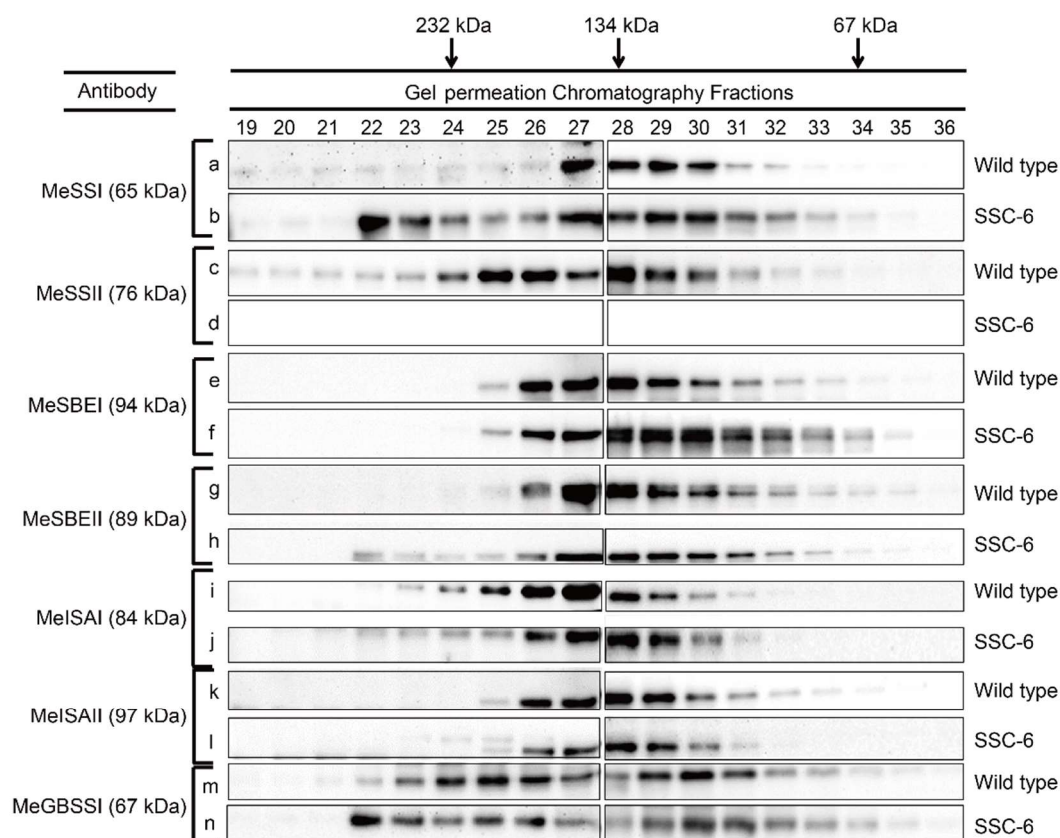
Figure 6

Figure 6. Characterization of protein interaction patterns and starch granule-bound proteins in storage roots between WT and SSC transgenic cassava plants.

(A) GPC analyses of proteins extracted from mature storage roots of wild type (WT) and SSC transgenic cassava plants. Proteins present in the indicated fractions from the GPC column were separated by SDS-PAGE and then probed with specific antibodies in immunoblot analyses. The

844   peak elution volumes of molecular mass standards analyzed using the same GPC protocol are

845   indicated at the top. The monomeric molecular weights of each enzyme are indicated on the left.

846   Material names are indicated on the right.

847   **(B)** Analysis of starch granule-bound proteins in storage roots of WT and SSC transgenic cassava

848   plants. Molecular mass standards are indicated on the left. The antibodies used for Western

849   blotting are indicated on the bottom. Sample names are indicated on the top. Arrowheads indicate

850   the bands that match the predicted molecular weights.

851

852   **Figure 7**

853
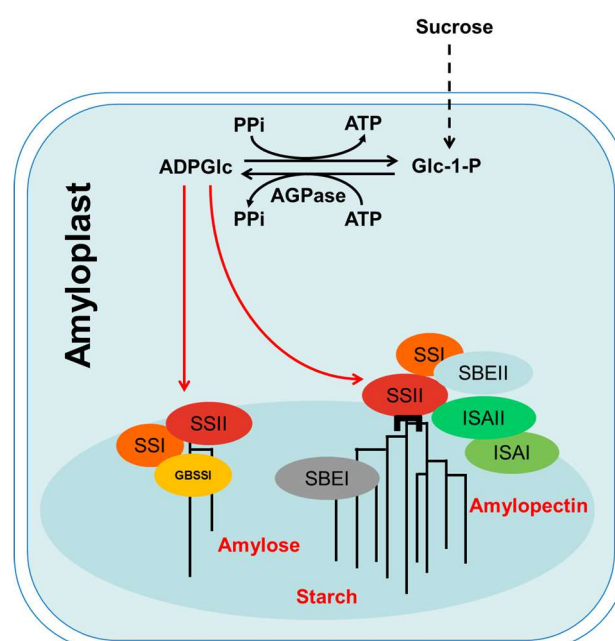
Figure 7. A molecular model of SSII function in starch biosynthesis in cassava storage roots.
SSII influences the assembly of heteromeric starch synthetic protein complexes and the starch binding ability of SSI, SBEII, ISAI, and ISAII through protein-protein interactions. Down-regulated *SSII* expression disrupts these protein complexes, which results in pronounced changes of starch properties in cassava storage roots.

859